A COMPARISON OF SYSTEM IDENTIFICATION TECHNIQUES FOR REFUGE TRACKING BEHAVIOR IN *EIGENMANNIA VIRESCENS*

by

Yu Yang

A thesis submitted to The Johns Hopkins University in conformity with the requirements for the degree of Master of Science in Engineering.

Baltimore, Maryland

June, 2020

Abstract

Mathematical modeling has commonly been used to represent various animal behaviors. However, for complex system such as sensorimotor process, explaining its dynamics by simple mathematical formulations would become very challenging. Therefore, the data-driven techniques could be used for the identification of animal behavior. In this study, we focus on comparing different data-driven techniques for system identification of refuge tracking response in the weakly electric glass knifefish (*Eigenmannia virescens*).

In the refuge tracking task, *Eigenmannia virescens* track a polyvinyl chloride refuge actuated in one degree of freedom via a motor which is controlled by a PC. The PC can give both deterministic signals (such as sum of sines and chirp) and stochastic signals (such as noise) to the system. Our data collection system allows simultaneous recording of movements of the refuge and the fish via a real-time image processing software. Given the input and output data, we estimated frequency response functions (FRFs) of the refuge tracking behavior by using non-parametric system identification techniques. Then, we used these FRFs to estimate parameters of parametric transfer function models for the behavior using parametric system identification techniques.

We investigated how the selection of input signals affect the frequency response function estimations. We then compared different mathematical models for the input–output behavioral response of the fish by using sum-of-sines type stimulus. We conclude the thesis by discussing the next steps of our research.

Primary Reader and Advisor: Noah J. Cowan

Second Reader: Ismail Uyanik

Acknowledgments

First and foremost, I'd like to express my gratitude to my advisor Dr. Noah J. Cowan for his kind guidance in my research path. His passion in research highly impressed me and his optimistic attitude towards life inspired me a lot.

Apart from my advisor, I want to appreciate Dr. Ismail Uyanik for his guidance as well. I developed not only practical skills and theoretical knowledge in research, but also the experience of how to manage the lab more proficiently during the years I worked with him in the lab.

I would like to thank our collaborator Dr. Eric S. Fortune for his previous excellent work in weakly electric glass knifefish which develops my interests in study of the fish refuge tracking behavior.

I also want to thank Balázs Vágvölgyi who put a lot of efforts on setting up the experimental apparatus before I joined the lab and was very patient to explain to me in detail what is going on in each part and help me with fixing the bug.

The Locomotion in Mechanical and Biological Systems (LIMBS) laboratory has not only helped me to improve my academic skills, but also has provided me a lot of good memories and a group of friends. Here I also want to thank other LIMBS lab members past and present: Dr. Robert W. Nickl, Dr. Manu S. Madhav, Dr. Ravikrishnan P. Jayakumar, Christopher Yang, Shahin Gharakozlou Lashkari, Debojyoti Biswas, Di Cao, Siming Deng, Michael Wilkinson, Jinwoo Choi, Dominic Yared, Bharath Krishnan, Brian Li, Marissa Ferreyros, Matthew Ma, Emily Sturm, James Hemker, Micaelle Larrieux, Yuqing Pan and Brittany Nixon.

I also want to thank Dr. Pablo A. Iglesias, my former faculty advisor in Electrical and Computer Engineering who gave me a lot of help and advice with courses I took and guided me to the control theory world.

I would also like to thank the staffs in Laboratory for Computational Sensing and Robotics (LCSR), Department of Electrical and Computer Engineering, and Department of Mechanical Engineering at Johns Hopkins University for their selfless assistance.

Last but not least, I want to express my huge gratitude to my parents Hong Yu and Zeyun Yang, who supported me both physically and mentally in my academic career, and to my late grandparents Xiufen Liu and Yongzhong Yu, who devoted their old age fostering new generation of our family, inspiring me to be honest, earnest and kind.

Dedication

This thesis is dedicated to my grandmother Xiufen Liu who performed as a supervisor in my early life, inspiring me with her great personality but passed away during my first year at Johns Hopkins University.

Contents

List of Tables

List of Figures

Chapter 1

Introduction

This thesis documents the work performed in the fulfillment of the degree of Master of Science in Engineering in Electrical and Computer Engineering in 2019. Small editorial corrections were made after the degree was conferred and the thesis is hereby published in its most up-to-date and accurate form.

System identification is a data-driven process, which allows obtaining analytical representations of dynamical systems based on experimental observations [1, 2]. The goal of this thesis is to apply system identification theory on an animal behavior towards understanding the underlying dynamics.

There is a vast literature on developing mathematical models to represent animal behavior [3]. Some of these modeling efforts, such as modeling the legged locomotion with spring–mass models, are quite successful in predicting center of mass trajectories of animal behaviors [4–7]. However, the modeling efforts get more and more complicated when the complexity of the system increases. For instance, it is very challenging to model the dynamics of sensorimotor processes with simple mathematical formulations. Therefore, this thesis focuses on data-driven techniques for identification of animal behavior. Specifically, we focus on system identification for refuge tracking response in the weakly electric glass knifefish (*Eigenmannia virescens*). We seek to compare a number of non-parametric and parametric system identification techniques in the literature to estimate the sensorimotor dynamics of *Eigenmannia virescens* during refuge tracking behavior.

In this chapter, we first give a brief description of system identification by describing some common procedures and techniques. We then continue by introducing our test animal, *Eigenmannia virescens*. Finally, we conclude the chapter with the explanation of refuge tracking behavior.

1.1 System Identification

The subject of system identification is concerned with the means and techniques for studying a process or system through observed or experimental data, primarily for developing a suitable (mathematical) description of that system [8–11]. Here we introduce the general procedures for system identification that are commonly used in the literature. The procedure of system identification mainly contains five steps.

The first step is data generation and acquisition [8]. The input-output data sets can be generated and recorded by conducting specifically designed system identification experiments. When designing system identification experiments, the inputs are of great significance: they need to be designed as rich as possible so that the output can reflect full information of the system.

Secondly is the data pre-processing step [8]. Usually, raw data collected during experiments cannot be directly used for the model estimation. Thus before they are presented to model estimation algorithms, the quality check and pre-processing steps should be implemented. Noises can be an obvious factor that influences data quality. Besides this, outliers, i.e. data which do not conform to other parts of the data because of the sensor breakdown and/or abrupt and brief process excursions, will also affect the quality of the data [8]. Therefore, pre-processing the data will be helpful for preparing cleaner data for next steps.

Thirdly is data visualization [8]. Data visualization is another step prior to the model development. It is an important step for extracting information and analysing signals, which can first give us an qualitatively confirmation to the data quality from an identification point of view [8]. It can also provide us primary information about the gain, delay, and dynamics of the system.

Besides, visualizing the time domain data in a transformed domain such as the frequency domain can also be beneficial since the spectrum or periodograms are very good methods for signal analysis [8].

Fourthly is model development [8]. Model development is the central goal of system identification. For each system, there can be a variety number of candidate models. When developing these candidate models, we first specify the model structure and order, then estimate the parameters of the model [8]. In practice, some model estimation toolboxes associated with data processing software such as Matlab can highly improve the efficiency of the model development.

Last but not least is model assessment and validation [8]. With many model candidates, we need to determine the best model guided by the data. Criteria should be followed or established for assessing the best model among candidates.

In practice, there are mainly two types of system identification methods. One kind of methods aims to use direct techniques to determine the transfer functions for a linear time-invariant system, rather than first select a confined set of possible models. Such methods are called *non-parametric* methods since they are data-driven and do not explicitly use parameters for the description [9]. Instead, if the parameters are estimated and models are built for the system identification, the methods are called *parametric*.

Parametric methods are model-based which possess a particular structure and order and have less number of unknowns than non-parametric methods which do not possess any structure or order. However, less prior knowledge is required when conducting non-parametric system identification while the estimation of parametric models demands some prior knowledge [8].

In this research, both of the two methods are used for system identification. A more detailed introduction to these two methods and how can they be realized in our research are included in Chapter 3 and Chapter 4.

Note that our research focuses on some common input signals and parametric models that have previously tested in similar studies. However, there are also many other techniques in the literature that can be used for the same purpose [12, 13].

1.2 *Eigenmannia virescens*

Eigenmannia virescens is a species of weakly electric glass knifefish which is widely distributed in the rivers of South America. Due to their natural refuge seeking behavior, these fish prefer to hide inside tree trunks or leaf litter in the wild in the light but they swim out in the dark [14–17].

Eigenmannia virescens, like most of the other species of weakly electric fish, generate electric currents to sense their surroundings in the dark and turbid waters [18]. The continuous production of these electric currents, known as electric organ discharge (EOD), generate electric fields around the body of the fish [19]. The weakly electric fish can be classified into two categories based on the way they generate this electric field: wave-type fish and pulse-type fish. The wave-type fish produce nearly sinusoidal electric currents at frequencies ranging between 200 Hz and 700 Hz [20]. The fish can sense the shape, size and distance of the objects nearby by using the reflections of this electric fields on their electroreceptors. These fish can also integrate the sensory information from electrosensory system with vision to obtain a more accurate representation of the environment [21]. This unique feature makes *Eigenmannia virescens* to be particularly special test animal to study multisensory integration and sensorimotor control [14, 21, 22].

Previous studies show that, as excellent maneuverable swimmers, *Eigenmannia virescens* also have a long, undulating ventral ribbon fin which is helpful for the generation of the propulsive force for locomotion [23]. The ribbon fin is composed of two inward-counterpropagating waves, one generated from their head and the other from their tail, meeting at a point called *nodal point* [22,24]. By adjusting the nodal point position at which the two waves meet, the fish can swim forward and backward equally well without reorienting their bodies.

Figure 1.1: *Eigenmannia virescens*, the "weakly electric glass knifefish". Photo credit: Will Kirk.

1.3 Refuge Tracking in *Eigenmannia* as a Feedback Control System

In the refuge tracking task, *Eigenmannia virescens* swims back and forth to keep its position inside a longitudinally moving refuge [17]. Fig 1.2 illustrates a block diagram representation of refuge tracking behavior in the form of a closed-loop feedback control model.

While it is clear [15] that this system possesses many rich and interesting nonlinearities, this research assumes that the refuge tracking behavior can be treated as a linear time-invariant (LTI) system. The input for the central nervous system (CNS) is the difference between the refuge movement and the self movement of the fish. We call this signal the sensory slip [14,25,26], represent-

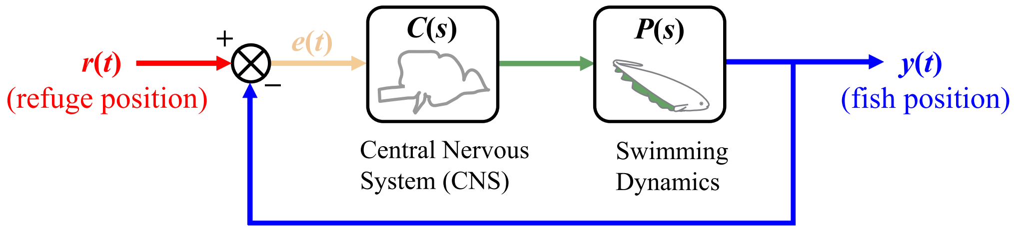

Eigenmannia virescens **Refuge Tracking System**

Figure 1.2: A block diagram representation of refuge tracking behavior. The input, refuge position, $r(t)$, and output, fish position, $y(t)$ were all baseline subtracted. The sensory slip $e(t)$ is the difference between system input and output as the input to the "controller" Central Nervous System (CNS). CNS will send control signal to the "Plant", the Swimming Dynamics for the locomotion.

ing the drift or error in tracking. Then, the CNS produces the control signals that stimulate the plant (swimming dynamics) to generate locomotion. The refuge tracking behavior has also been studied before and its linear functioning regimes has been described [15]. Therefore, we will perform our experiments in a similar input–output regime to ensure LTI response of the system for further analysis.

Chapter 2

Experimental Environment and Apparatus

2.1 Experimental Environment

Adult *Eigenmannia virescens* (10–15 cm in length) were obtained through commercial vendors and housed according to the guidelines [27] previously published. The experimental tanks were maintained with a water temperature around 78°F and conductivity in the range of 10–150 μS/cm. All the experiments were conducted in the illumination in the range (300–500 lux) and all experimental procedures were approved by the Johns Hopkins Animal Care and Use Committee and followed guidelines established by the National Research Council and the Society for Neuroscience.

2.2 Experimental Apparatus

The methods are from Biswas et al [25], and are only briefly described here. For full details, please see [25]. The experimental apparatus is similar to that reported in previous studies [14–16, 21, 25, 28]. The test environment is a 17 gallon rectangular glass tank. A heater is placed inside the water to maintain the temperature and air filter is connected to the air sources providing oxygen for the environment. The refuge was machined from a 152 mm (152.49±0.28) segment of 46.64×50.65 (46.64±0.33×50.65±0.10) mm gray rectangular PVC tubing, with the bottom surface of the tube removed. Both sides of the refuge were machined with a series of six rectangular windows (with a width of 6 mm and spaced 19 mm apart) to provide visual and electrosensory cues.

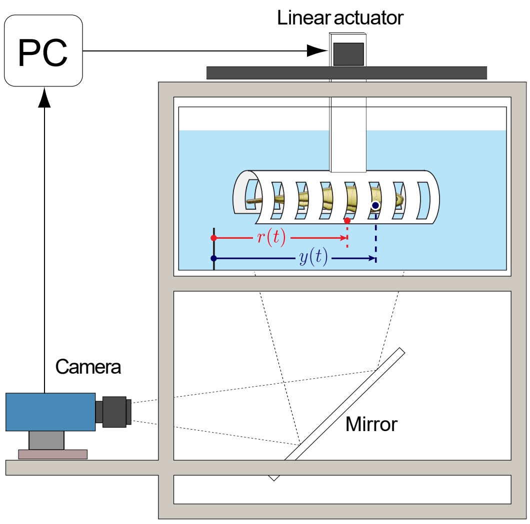

Figure 2.1: Experimental Apparatus

A PC gives the designed input signal to the refuge actuated by a stepper motor, leading to the one degree of freedom refuge moving in real time. The high-resolution camera captures the real time refuge and fish image by mirror reflection and transfers the image to a Labview PC. Template matching is employed in Labview to determine the real-time position of the fish for time-domain data collection. After each trial, both the input refuge position $r(t)$ and the output fish position $y(t)$ are saved in PC.

Chapter 3

Non-parametric System Identification of Refuge Tracking Behavior

Our goal is to do system identification of fish refuge tracking behavior. In this chapter, we introduce the non-parametric system identification for refuge tracking behavior. Non-parametric system identification means estimating the frequency response characteristics of a system relying on the input and output data without mathematical modeling. Since it is a data-driven process, it is very crucial to design input signals rich enough so that the input can trigger different dynamics of the system for us to observe the response in the output. Then the frequency response characteristics can be estimated by using the input and output.

In our research, we designed three different input signals with rich frequency contents. All of them would be extremely helpful for frequency domain analysis but also require different methods when processing the data. By comparing the results of different input stimuli, we could find the best stimulus and the best data processing method for data with that stimulus, preparing for model-based system identification.

3.1 Experimental Stimuli

Our Experimental Stimuli could be classified as two types. One is called *Deterministic Input*. The other is called *Stochastic Input*. Deterministic input has a completely known physical description, whereas stochastic input is not deterministic, which includes noise.

3.1.1 Sum of sines

First stimulus we tested was sum of sines, which has also previously been used for identification of refuge tracking response of the fish [15]. It is a kind of deterministic input, including 13 single sinusoidal signals at different frequencies, written as below:

$$r_1(t) = \sum_{i=1}^{13} \frac{1}{0.1\pi k_i} \cdot \cos(0.1\pi k_i t + \Phi_i), \tag{3.1}$$

where $k_i = 2, 3, 5, 7, 11, 13, 17, 19, 23, 29, 31, 37, 41$ are prime numbers to prevent harmonics in the input stimuli. From Eq. (3.1), we can find that the frequency of each single sinusoidal component was designed to be $2\pi \times 0.05 \times k_i$. Then the sum of sines input has a period of 20 s. The amplitude of each single sinusoidal signal was inversely proportional to its own frequency in order to ensure constant velocity magnitude, while phases Φ_i were randomized for each frequency components. The total sum of sines stimulus duration we designed was 40 s, twice of the period of sum of sines.

3.1.2 Chirp

We then implemented a chirp type stimulus signal, which has previously been used for identification of legged locomotion [29]. Chirp stimulus we implemented were also a sort of deterministic input. It is a 40-second sinusoidal signal, logarithmically increasing its frequency from 0.05 Hz to 2 Hz but linearly decreasing its amplitude from 0.05 m to 0.001 m. The equation of chirp stimulus is as follows:

$$r_2(t) = (\alpha t + a_0) \cdot \sin\left(2\pi f(t)\right). \tag{3.2}$$

In Eq. (3.2),

$$\alpha = \frac{a_1 - a_0}{t_1 - t_s},$$

$$f(t) = \frac{t_1}{\ln(\frac{f_1}{f_0})} \cdot \left(f_0 \cdot \left(\frac{f_1}{f_0}\right)^{\frac{t}{t_1}} - f_0\right),$$

where a_0 = 0.05 m, a_1 = 0.001 m, t_1 = 40 s, t_s = 0.04 s, f_0 = 0.05 Hz, f_1 = 2 Hz, t_s represents the sampling time and $\ln(\cdot)$ represents the natural logarithm of a number.

3.1.3 Noise

We also tested with noise type input signal, which is a type of stochastic stimulus and previously used for identification of legged locomotion [30].

Here we first generated a vector of random numbers in a length of 1000, uniformly distributed between -0.2 and 0.2. Then we transferred these random numbers into frequency domain by computing Discrete Fourier Transform (DFT) and cut off all the frequency components bigger than equal to 2.05 Hz. After that, in frequency domain, at each remaining frequency component f_m, the signal was multiplied by $\frac{1}{(2\pi f_m)^{\frac{3}{4}}}$. Finally we transferred the signal back to time domain and got our noise stimulus with frequency components between 0 Hz and 2.05 Hz. The duration of this noise stimulus was 40 seconds.

3.2 Experimental Procedure

Each fish $(N = 3)$ were tested individually. Each fish was transferred to the experimental tank and allowed to acclimate for 2 – 12 hours prior to the start of the experiment.

For each fish, the experiments with three stimulus were conducted in one day. First, we performed 5 – 10 trials of the sum of sines experiment, then 5 – 10 trials of chirp experiment and 5 – 10 trials of noise experiment in the end, all in light environment. Each trial lasts 70 seconds in total. One-minute breaks were given between two consecutive trials for the fish to have rest. We took experimental notes for every trial of the experiments with each fish, describing the observation of the fish performance during that trial, such as tracking loss happened during the experiment, since template matching was used to track the fish position.

3.3 Data Analysis

Time domain refuge and fish trajectories, $r(t)$ and $y(t)$ accordingly, were automatically digitized with the sampling rate 25 Hz and saved in the PC of the experimental apparatus.

In the data pre-processing step, for the data we got from each trial with each fish, the first 20 seconds and last 20 seconds of input and output raw data (including those in the first 10 seconds of ramping-up period for sum of sines and noise input case) were discarded to get purer, cleaner data for further analysis. Besides, we subtracted baseline so that the initial position of the refuge and that of the fish relative to the refuge couldn't make any difference. Outlier experiments were eliminated based on the experimental notes.

Then for each individual fish, we observed time domain trajectories of all the trials and eliminated other outlier experiments. Then we averaged the fish trajectories in time domain. Next step was to use a common way for non-parametric system identification such as Empirical Transfer Function Estimate (ETFE) to estimate the FRF of the refuge tracking system. Primarily, we used Discrete Fourier Transform (DFT) to transfer the time domain input $r(t)$ and output $y(t)$ to the frequency domain as complex-valued functions of frequency, $R[\omega]$ and $Y[\omega]$. The DFT computations are as follows:

$$R[\omega] = \sum_{t=1}^{N} r(t)e^{-j\omega t}, \tag{3.3}$$

$$Y[\omega] = \sum_{t=1}^{N} y(t)e^{-j\omega t}, \tag{3.4}$$

where $\omega = 2\pi k/N$, $k = 1, 2, 3, \ldots, N$.

Then the ETFE $\hat{G}(e^{j\omega})$ can be calculated by

$$\hat{G}(e^{j\omega}) = \frac{Y[\omega]}{R[\omega]}. \tag{3.5}$$

The Eq (3.5) means that ETFE can be computed at each frequency component of input and output in frequency domain. This computation provides a set of complex numbers, which represent the estimation of FRF at each corresponding frequency. However, we need to be careful that ETFE was not defined when the denominator term $R[\omega]$ = 0.

3.4 Results

3.4.1 Refuge Tracking Performance of *Eigenmannia virescens* in Time Domain

After outlier detection with notes, we put all trials of output data together with their average in the same figure, and compared the average with the input stimulus during that period. Fig 3.1, Fig 3.2, Fig 3.3 indicate the fish tracking performance in time domain.

In sum of sines input case, since the input signal was the summation of multi-frequency sinusoidal signals, it stimulated a broad range of dynamics because of the high frequency components. The Fig 3.1 shows that the fish could track the low frequency components of sum of sines input very well, but may not track the high frequency components as well as it does for low frequency components.

In chirp input case, the input is a signal with logarithmically increased frequencies but linearly decreased magnitude. As shown in Fig 3.2, the fish could also perform their tracking well at low and medium frequencies, but again could not track the high frequency very well.

In noise input case, we noticed from Fig 3.3 that the fish could track the noise dynamics well, but at the same time, didn't move as much as the refuge

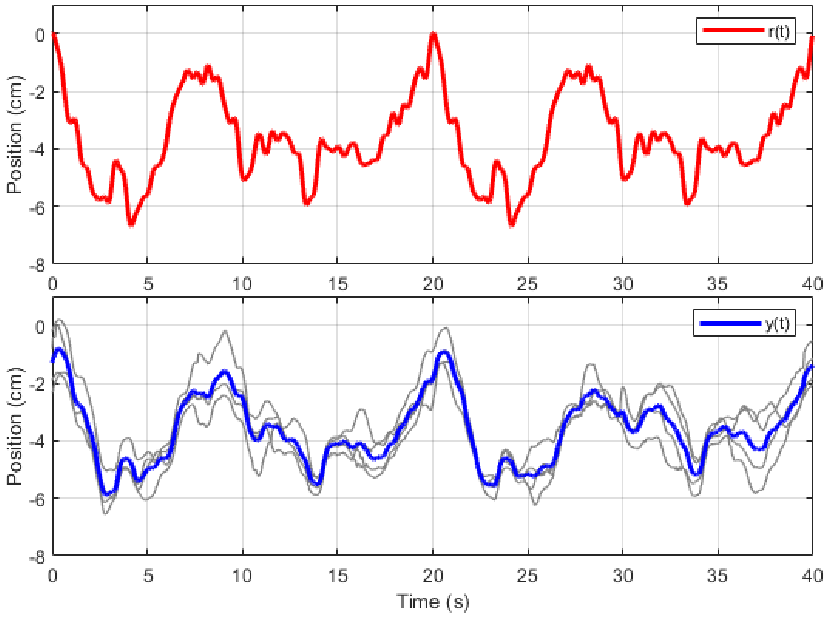

Figure 3.1: Sum of sines input signal $r(t)$ at $t = 0 - 40s$ (in red color) and corresponding output fish position $y(t)$ (in blue color). Take one fish data (out of $N = 3$) as an example.

moved during the experiments.

3.4.2 Issues with the Estimation of True FRF Using ETFE

Tracking performance of the fish in time domain will dramatically influence the frequency domain analysis. Ideally, assume that the fish could track the refuge movement exactly the same magnitude without any time delay, then we will get a Bode plot with gain to be one and zero phase at all frequencies. However, the fish tracking system cannot be an ideal system like that, so at

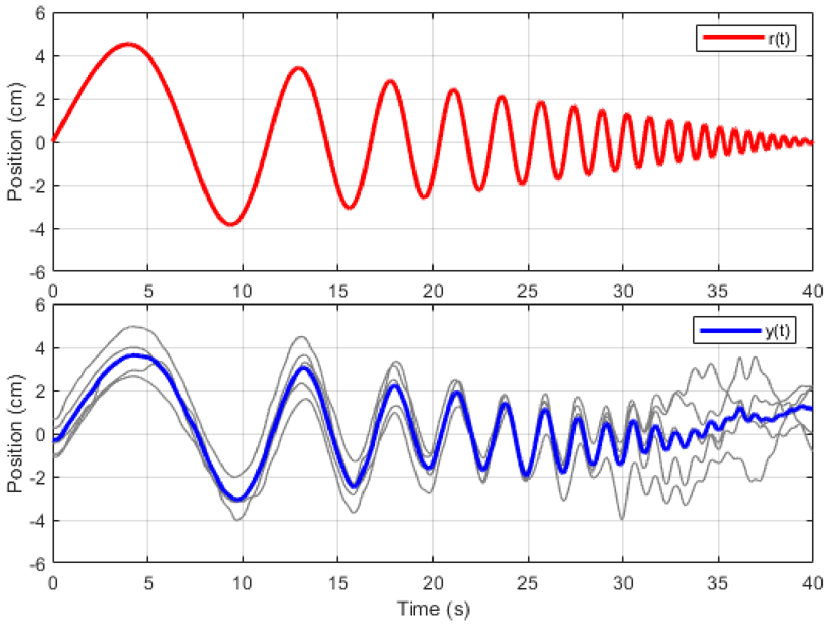

Figure 3.2: Chirp input signal $r(t)$ at $t = 0 - 40s$ (in red color) and corresponding output fish position $y(t)$ (in blue color). Take one fish data (out of $N = 3$) as an example.

some frequencies, the response would have a lower gain and more phase lag. In the sum of sines input case, as our hypothesis, the fish tracking system is an LTI system, which means that if the input has 13 frequency components, the output should also be composed of exactly these 13 frequency components. So in our case, we plotted the frequency domain amplitude of input in Fig 3.4 and found that the input only had 13 spikes at each frequency components. We could also clearly observe spikes at those 13 frequencies in the output frequency domain amplitude plot Fig 3.5. So ETFE would be defined at all these 13 frequencies and the estimation results were 13 complex numbers.

The Bode plot Fig 3.6 was drawn by those 13 complex numbers we got from

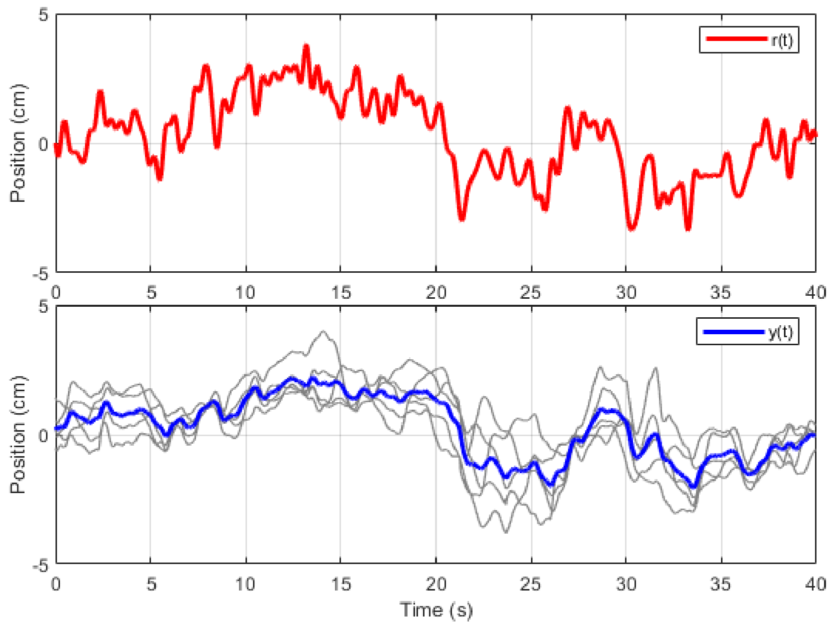

Figure 3.3: Noise input signal $r(t)$ at $t = 0 - 40s$ (in red color) and corresponding output fish position $y(t)$ (in blue color). Take one fish data (out of $N = 3$) as an example.

ETFE results. Here we could also interpolate the FRF at other frequencies by connecting the adjacent two frequencies among all 13 of them because we didn't design the input signal at those frequencies for sum of sines case. And the time domain tracking performance has already shown that the fish couldn't track the dynamics of high frequency components that perfect. So in Bode plot Fig 3.6, we witnessed that although at low frequency, the gain of fish was close to 1 and the phase lag was very low, as frequency increasing, the gain had a trend of decreasing and phase lag tended to rise up.

Since the sum of sines stimulus only contained 13 frequency components, other frequency components would merely be interpolated based on ETFE com-

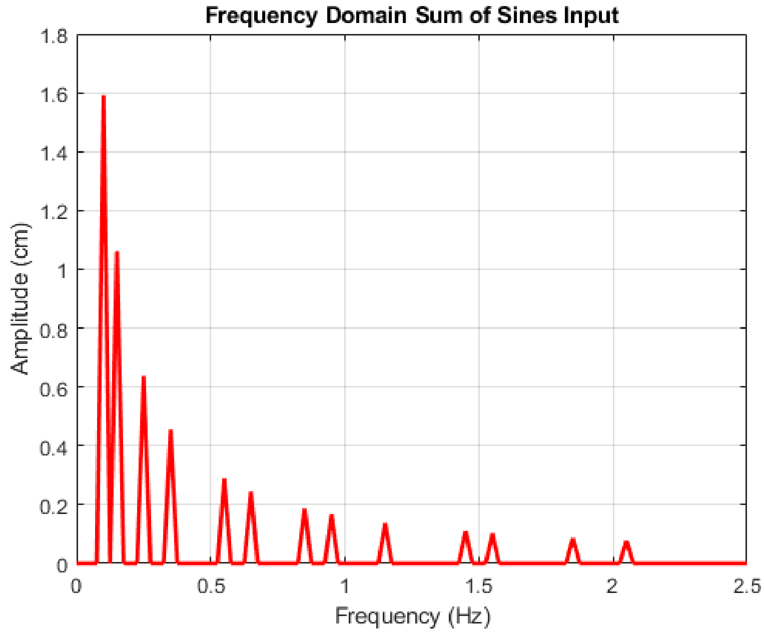

Figure 3.4: Frequency domain amplitude of sum of sines input signal. Clearly witnessed 13 spikes at each frequency component. Take one fish data (out of $N = 3$) as an example.

puted at existed frequencies in sum of sines case. These interpolation might be less accurate than directly computation by ETFE. So this is a disadvantage for a stimulus with not too many frequency components such as our designed sum of sines.

But the chirp stimulus contained more frequencies than sum of sines. We could compute ETFE at all frequencies in the range of 0.05 Hz to 2 Hz with frequency resolution of 0.025 Hz rather than interpolate FRF from a small number of frequencies. Again, the Bode plot could be drawn at these frequencies in Fig 3.7.

From Fig 3.7 we can see that both the gain and phase decrease but have

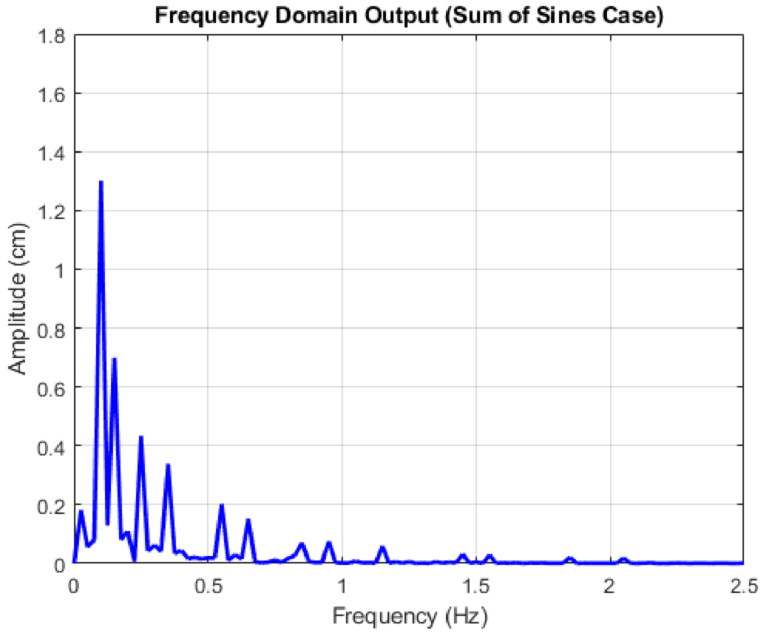

Figure 3.5: Frequency domain amplitude of fish output corresponding to sum of sines input. Here we also witnessed 13 spikes at same corresponding frequencies of sum of sines input. Take one fish data (out of $N = 3$) as an example.

more oscillations as frequency increasing.

Similarly, the noise stimulus we designed was composed of more frequency components than the other two stimuli. If we followed the same process we did for the sum of sines and chirp case, we could get Bode plot for the noise input case in Fig 3.8.

From the Fig 3.8 we can see that the noise input case has a very messy Bode plot. Oscillations happen a lot at all frequencies, but more severe at high frequency parts.

Based on the observation of Bode plot for three kinds of inputs, we could observe that the Bode plot were not smooth in both chirp and noise input case.

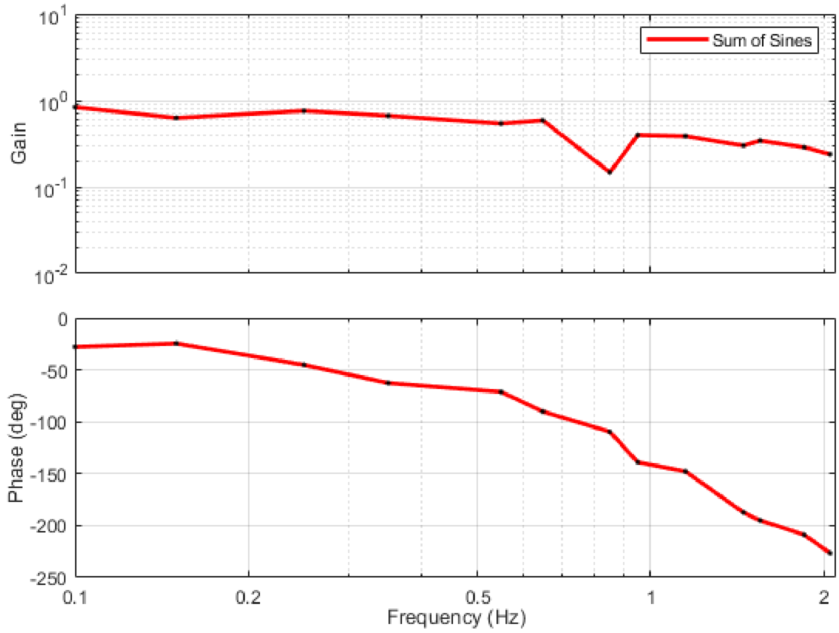

Figure 3.6: Bode plot of the sum of sines input case by ETFE at 13 frequency components and interpolation at other frequencies. Take one fish data (out of $N = 3$) as an example.

However, for a physical system, the Bode plot should definitely be smoother than the plot we got. So we found that actually ETFE has an issue about the estimation of FRF for refuge tracking system.

In order to dig out the reason that bring about the issue of inaccurate estimation of ETFE, we had to study the properties of ETFE.

First, consider a system S with actual FRF $G_0(q)$, given an input $r(t)$, there is a stochastic disturbance $v(t)$ with zero mean before the output $y(t)$. Then the relationship between input and $r(t)$ output $y(t)$ is:

$$y(t) = G_0(q)r(t) + v(t). \tag{3.6}$$

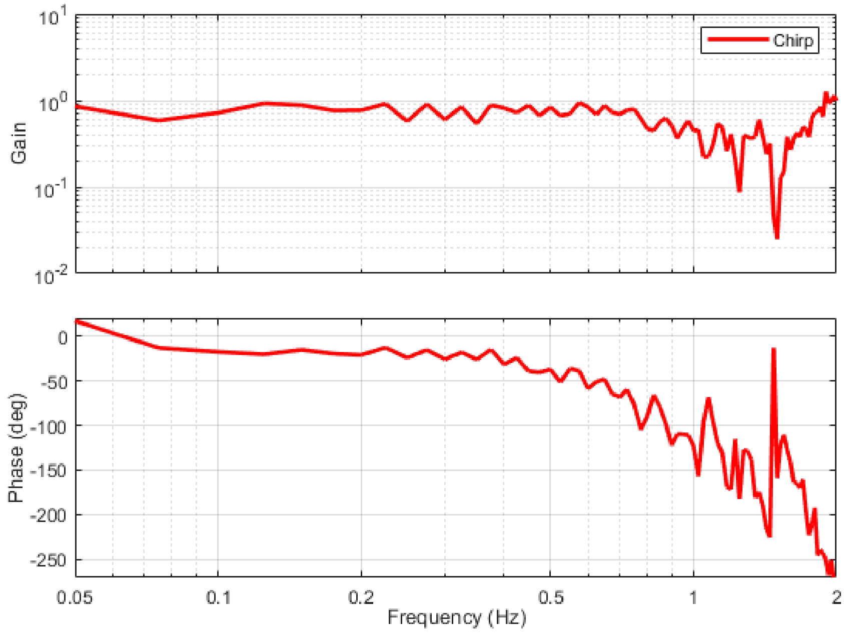

Figure 3.7: Bode plot based on ETFE for the chirp stimulus case with the frequency range of 0.05 Hz – 2 Hz. The frequency resolution is 0.025 Hz. Take one fish data (out of $N = 3$) as an example.

Because of the stochastic disturbance term corrupting the data, the ETFE of a system, which is the estimation would be a random variable. That means, for different experiments, ETFE is different.

Second, ETFE is computed at a variety of frequencies. But there is no correlation between estimation at the frequency ω_k and the other frequencies, such as ω_{k-1} and ω_{k+1}.

Third, at one frequency ω_k , the estimate is a random variable distributed around the actual $G_0(e^{j\omega_k})$ because the disturbance term $v(t)$ has zero mean.

So the ETFE will be more reliable if the variances of the estimates are small for all ω_k.

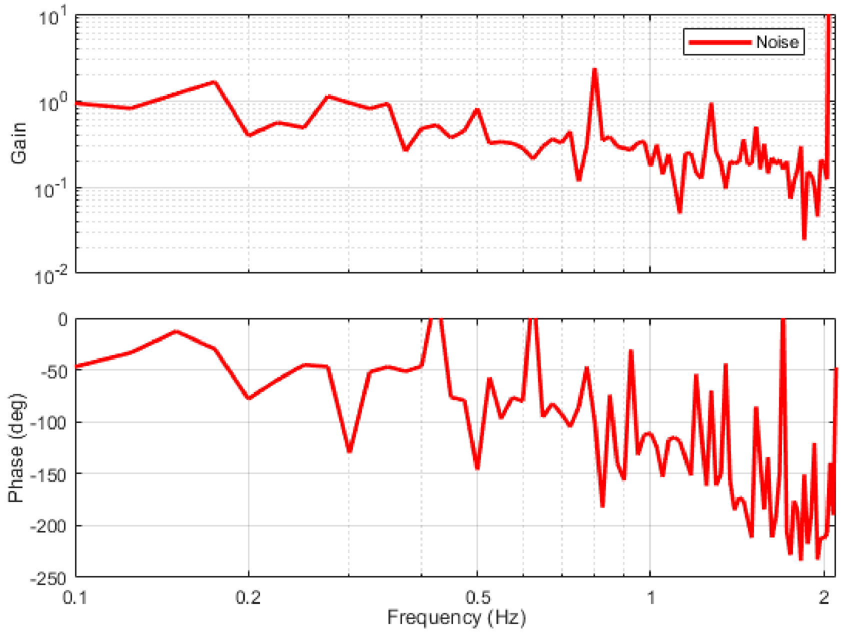

Figure 3.8: Bode plot based on ETFE for the noise stimulus case. Take one fish data (out of $N = 3$) as an example.

For the system S with zero-mean disturbance term $v(t)$, we could compute its DFT $V[\omega]$,

$$V[\omega] = \sum_{t=1}^{N} v(t)e^{-j\omega t}. \tag{3.7}$$

Then, transfer the Eq (3.6) in freuqency domain,

$$Y[\omega] = G_0(e^{j\omega})R[\omega] + Q[\omega] + V[\omega]. \tag{3.8}$$

Here, based on Theorem 2.1 in [9], $Q[\omega]$ is the error incurred in the approximating the exact FRF with a finite-sample version and bounded with $1/\sqrt{N}$ and will decay as the number of samples N increases.

Then, FRF can be estimated as

$$\hat{G}(e^{j\omega}) = G_0(e^{j\omega}) + \frac{Q[\omega]}{R[\omega]} + \frac{V[\omega]}{R[\omega]}. \tag{3.9}$$

Since we know that the variance of the estimated FRF is

$$\begin{aligned} var\Big[\hat{G}(e^{j\omega})\Big] &= cov\Big(\hat{G}(e^{j\omega}), \hat{G}(e^{j\omega})\Big) \\ &= E\Bigg[\bigg(\hat{G}(e^{j\omega}) - E\Big[\hat{G}(e^{j\omega})\Big]\bigg)^2\Bigg], \end{aligned} \tag{3.10}$$

By assumption, $E\Big[V[\omega]\Big] = 0, \quad \forall\omega$

$$E\Big[\hat{G}(e^{j\omega})\Big] = G_0(e^{j\omega}) + \frac{Q[\omega]}{R[\omega]}. \tag{3.11}$$

Thus, we can get

$$\hat{G}(e^{j\omega}) - E\Big[\hat{G}(e^{j\omega})\Big] = \frac{V[\omega]}{R[\omega]}. \tag{3.12}$$

So the variance of estimated FRF is

$$\begin{aligned} var\Big[\hat{G}(e^{j\omega})\Big] &= E\Bigg[\bigg(\hat{G}(e^{j\omega}) - E\Big[\hat{G}(e^{j\omega})\Big]\bigg)^2\Bigg] \\ &= E\left[\frac{\big|V[\omega]\big|^2}{\big|R[\omega]\big|^2}\right]. \end{aligned} \tag{3.13}$$

For deterministic input signals $r(t)$ (such as sum of sines signal and chirp signal):

$$E\left[\left|R[\omega]\right|^2\right] = \left|R[\omega]\right|^2. \tag{3.14}$$

Then the variance of estimated FRF can be written as

$$var\left[\hat{G}(e^{j\omega})\right] = \frac{E\left[\left|V[\omega]\right|^2\right]}{\left|R[\omega]\right|^2}. \tag{3.15}$$

We could let $E\left[\left|V[\omega]\right|^2\right] \approx \Phi_v(\omega)$, $\Phi_v(\omega)$ is the spectrum of $v(t)$ [9]. Then we can get this expression:

$$var\left[\hat{G}(e^{j\omega})\right] \approx \frac{\Phi_v(\omega)}{\left|R[\omega]\right|^2}. \tag{3.16}$$

For stochastic input signals $u(t)$ (such as noise signal):

$$var\left[\hat{G}(e^{j\omega})\right] = \frac{E\left[\left|V[\omega]\right|^2\right]}{E\left[\left|R[\omega]\right|^2\right]}. \tag{3.17}$$

Again, $E\left[\left|V[\omega]\right|^2\right] \approx \Phi_v(\omega)$, $\Phi_v(\omega)$ is the spectrum of $v(t)$; $E\left[\left|R[\omega]\right|^2\right] \approx \Phi_r(\omega)$, $\Phi_r(\omega)$ is the spectrum of $r(t)$ [9]. Then get this approximation expression:

$$var\left[\hat{G}(e^{j\omega})\right] \approx \frac{\Phi_v(\omega)}{\Phi_r(\omega)}. \tag{3.18}$$

First look at our sum of sines input case:

$$r_1(t) = \sum_{i=1}^{13} \frac{1}{0.1\pi k_i} \cdot \cos(0.1\pi k_i t + \Phi_i),$$

where $k_i = 2, 3, 5, 7, 11, 13, 17, 19, 23, 29, 31, 37, 41$, the ETFE is only computed at $\omega_k = 0.1\pi k_i$. Based on Eq (3.16), $\left|R[\omega]\right|^2$ could be computed at ω_k, based on the results of example 2.1 in [9], we can get:

$$\left|R[\omega_k]\right|^2 = \frac{NA_k^2}{4}. \tag{3.19}$$

A_k is the amplitude of the sinusoid at ω_k. Thus, the variance of ETFE at the available frequencies ω_k is:

$$var\left[(\hat{G}(e^{j\omega_k})\right] \approx \frac{\Phi_v(\omega_k)}{\left|R[\omega_k]\right|^2} = \frac{4\Phi_v(\omega_k)}{NA_k^2}. \tag{3.20}$$

So the variance of ETFE can decay as N and A_k increase [9].

Then look at the stochastic input case, such as our noise input case. If we know the variance of noise input is σ_r^2. The variance of ETFE at the available frequencies ω_k can be estimated by:

$$var\left[(\hat{G}(e^{j\omega_k})\right] \approx \frac{\Phi_v(\omega_k)}{\Phi_r(\omega_k)} = \frac{\Phi_v(\omega_k)}{\sigma_r^2}. \tag{3.21}$$

Note $\sigma_r^2 \ll NA_k^2$ since power of our sum-of-sines signal is concentrated in just a few signals [9].

Based on the above discussion, the reason why ETFE does not perform very well for stochastic signals is that the estimation is random, and variance of estimation is high. To improve our estimation, we can decrease the variance of ETFE by increasing sample size or magnitude of input signal for deterministic input case. However, this method is not quite useful when the input is stochastic.

3.4.3 Smoothing Window in ETFE Could Improve the Estimation for Stochastic Stimulus Case

From the last section we know that when the input is stochastic signal, the variance of ETFE cannot be decreased by lifting sample size or increasing the input amplitude. So we tried to implement more methods to improve the estimation. One idea was to use smoothing window in ETFE.

Matlab uses Hamming window for the smoothing of their "etfe" command.

Fig 3.9, Fig 3.10, and Fig 3.11 illustrate the comparison between original ETFE and smoothed ETFE for each case using Hamming Window in matlab "etfe" command.

For sum of sines input case, we can find that the Hamming smoothing window didn't affect the estimation very much. The smoothing window really smoothed oscillation of the gain and phase in chirp input case but keep the trend to be similar, which suggests that the smoothing windows can actually improve the estimation of deterministic input case as well. For the noise input

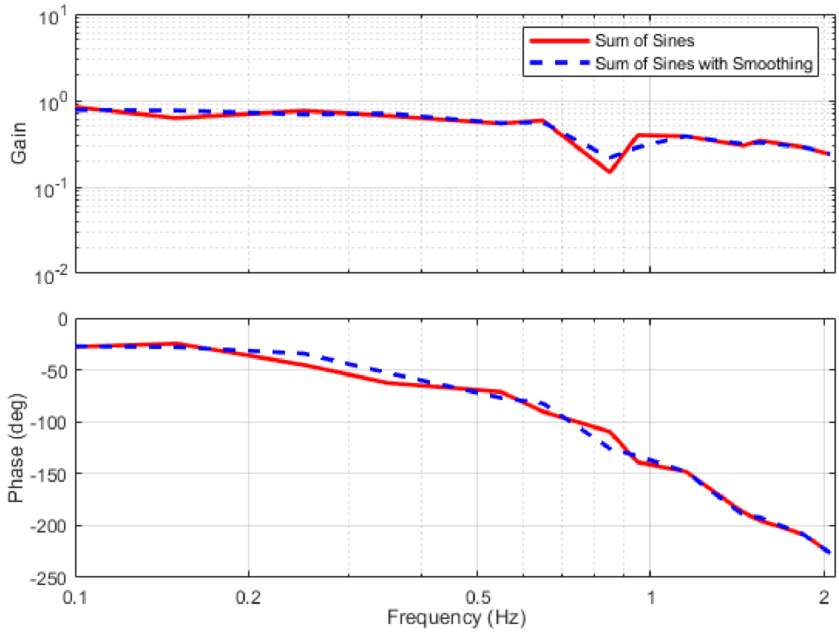

Figure 3.9: Bode plot based on ETFE for the sum of sines stimulus case and that smoothed with Hamming Window. Take one fish data (out of $N = 3$) as an example.

case, in the Fig 3.11, the smoothing window had a strong impact on the case, which dramatically decreased variances of the original ETFE estimation.

The principle of smoothing window is that it can reduce the variance by averaging over neighbouring frequency points. Smoothing is motivated by two important ETFE properties. First of all, ETFE estimations are independent for different ω_k. Besides, averaging over a frequency area where $G_0(e^{j\omega})$ is constant reduces the variance.

A Hamming window was what used to smooth the ETFE. But an important thing that should be noticed is that there is bias/variance trade-off. Windowing introduces bias while reducing the variance. And we need to be careful to

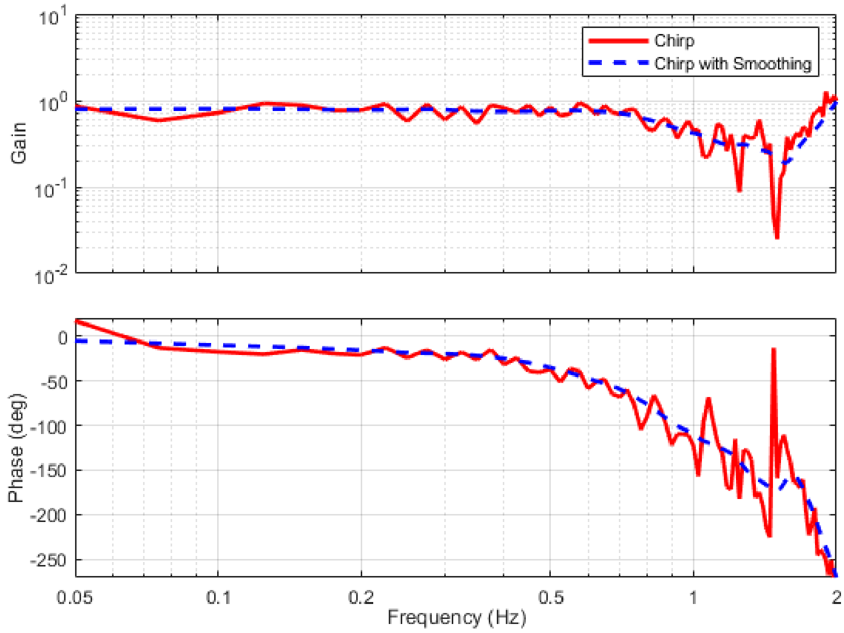

Figure 3.10: Bode plot based on ETFE for the chirp stimulus case and that smoothed with Hamming Window. Take one fish data (out of $N = 3$) as an example.

choose window sizes. If the window is too narrow, the variance is still too large. If the window is too wide, it may also smooth the dynamic.

3.5 Discussion

Following our hypothesis, if the refuge tracking system is an LTI system, then no matter what the stimulus is, the FRF would not change. That means we should obtain the same Bode plot for all three cases. However, based directly on computation of ETFE in all three input cases, we found that these three estimates of FRF vary a lot (see Fig 3.12). But we could not tell whether

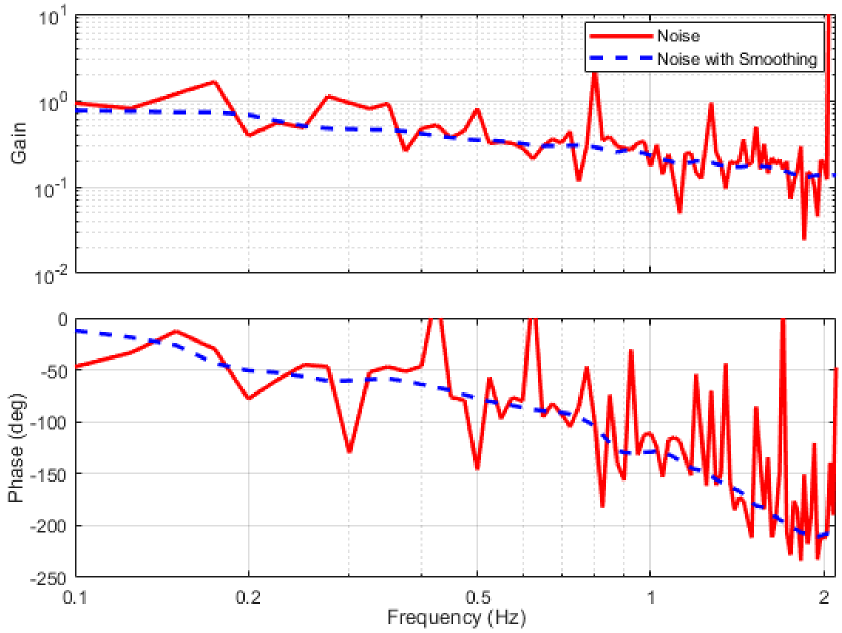

Figure 3.11: Bode plot based on ETFE for the noise stimulus case and that smoothed with Hamming Window. Take one fish data (out of $N = 3$) as an example.

the difference comes from fish refuge tracking system itself or not since the disturbance noises during experiments caused high estimation variances with ETFE method in chirp and noise input cases. Besides, "windowing artifact" for chirp and noise inputs could also result in the imperfect FRF estimations with ETFE method because the spectral leakages occur across frequencies for these non-periodic stimuli. The periodic sum of sines stimulus wouldn't be effected by windowing artifact since the length of data for processing was perfectly chosen as multiples of the period of the input. Thus we applied smoothing window to improve the estimation of ETFE in three input cases and compared the results (Fig 3.13). From the Fig 3.13, all these three estimates generally follow the trend of decreasing gain and more phase lag as frequency increasing. But we still observed that the FRF estimation in chirp input case has an “rise-up” gain at above 1 Hz. Besides, the estimation of FRF from chirp input case has the smallest phase lag and that from noise input case has the lowest gain at most frequencies within the frequency range 0.1 Hz – 2 Hz. These results suggest the nonlinearity of the refuge tracking system of *Eigenmannia virescens* across different stimulus cases. The possible reason could be related to but not restricted to the stimulus predictability [15] and amplitude saturation.

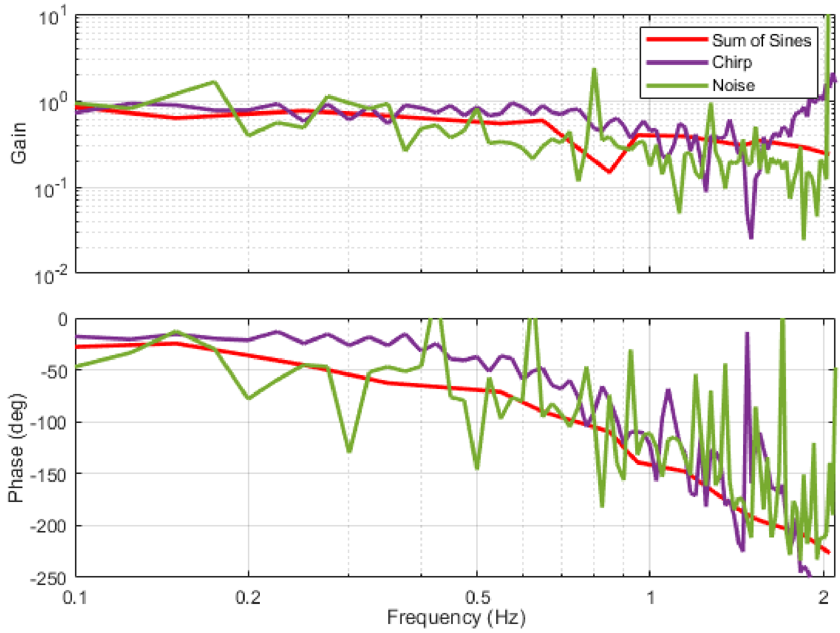

Figure 3.12: Bode plot based on ETFE for all three stimulus cases. Take one fish data (out of $N = 3$) as an example.

All in all, the ETFE itself might not provide us a good estimate. However, we were able to improve the estimation performance of ETFE. For the deterministic stimulus, the ETFE results could be improved by increasing the sam-

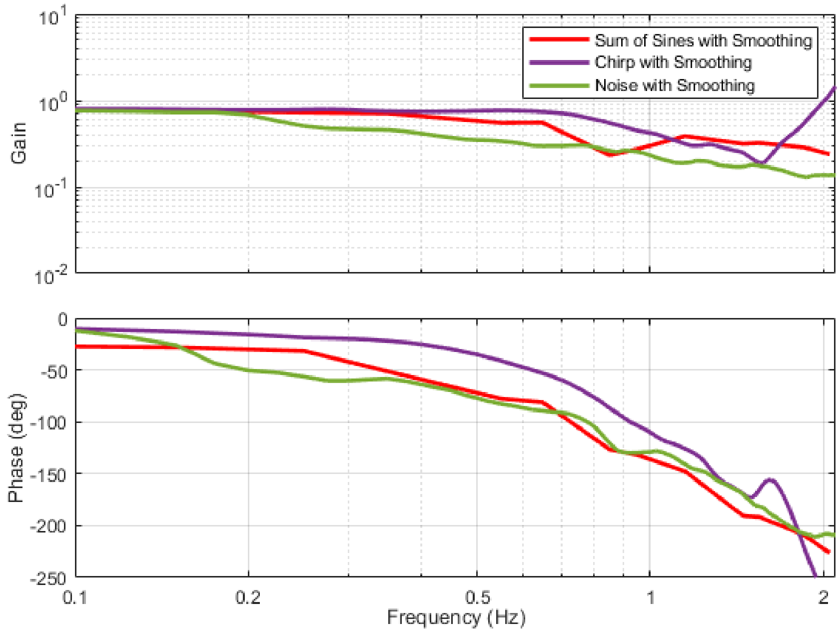

Figure 3.13: Bode plot based on ETFE for all three stimulus smoothed with Hamming Window. Take one fish data (out of $N = 3$) as an example.

ple size and input amplitude or applying smoothing windows. For the stochastic stimulus, smoothing windows could be used for getting a better estimation. However, among the three cases, since the fish would have more predictable movement when tracking the chirp input, the smoothing window size would be hard to be chosen for the noise case, we would choose the sum of sines input for the parametric system identification.

Chapter 4

Parametric System Identification of Refuge Tracking Behavior

Parametric system identification is a technique which allows fitting mathematical models to input output data. Here, we used non-parametric system identification results, such as ETFE, and then estimate the parameters of the parametric models based on the ETFE. Our idea of parametric system identification for fish refuge tracking system was to input the ETFE (complex numbers) results to the System Identification Toolbox in Matlab for the initial fitting and then manually adjusted the parameters of the model to get a better fitting visualized in Bode plot.

We took different approaches in modeling the refuge tracking system depicted in Fig 1.2. As seen from the Block Diagram, the refuge tracking system has a closed-loop model with Controller (transfer function $C(s)$, abbreviated as C here), Plant (transfer function $P(s)$, abbreviated as P here) and a unit negative feedback. First we obtained a model for the closed-loop transfer function, noted as G here. Then we modeled the inner loop CP (the multiplication of transfer function C and P) directly from input output data.

In parametric system identification part, we use frequency response function estimations obtained through sum of sines input signals, a sample of which is illustrated in Fig 4.1, since they provide accurate and intuitional Bode plots as shown in the results of Chapter 3.

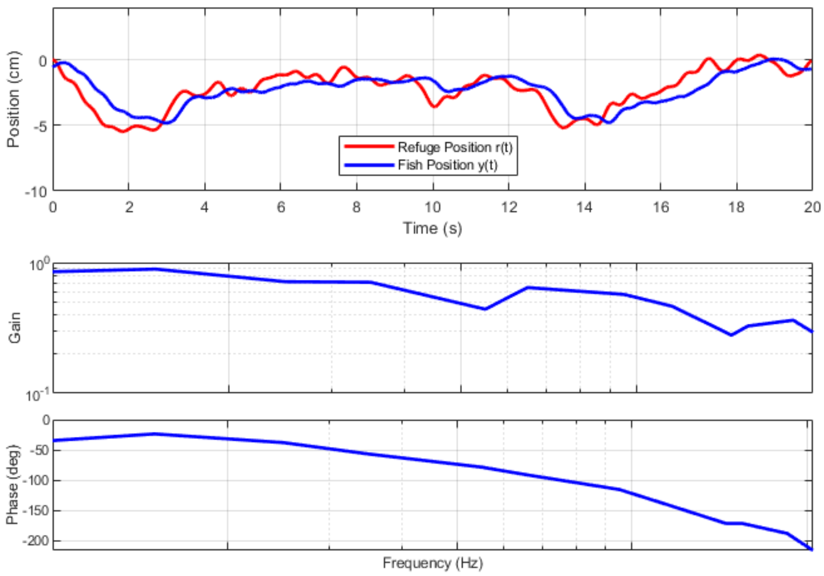

Figure 4.1: Sampled trial with one fish (out of $N = 4$), containing the time-domain input (red color) and output (blue color) plot on the top and Bode plot (both gain and phase) at bottom.

4.1 Models

Just as mentioned in Chapter 1, Model development was the central goal for system identification. So in this section, we introduce the process of developing three model candidates and make a discussion about these models.

4.1.1 The Canonical Second Order Transfer Function Model with Time Delay

Following the previous efforts on identifying the refuge tracking performance of these fish [16,24], we used a canonical second order transfer function model as our base parametric form. These type of second order models are also common in engineering applications such as the mass-spring-damper system and RLC circuit. In Laplace domain, the transfer function of canonical second order system, noted as $G(s)$, can be written as following:

$$G(s) = \frac{K{\omega_n}^2}{s^2 + 2\xi\omega_n s + {\omega_n}^2}. \tag{4.1}$$

So we initially imported the complex values of ETFE, frequencies corresponding to these complex values as well as the sampling time to the system identification toolbox, the interface of which is in Fig 4.2, then estimated the transfer function model with two poles and no zeros. We could get an initial canonical second order model estimation of the fish refuge tracking system.

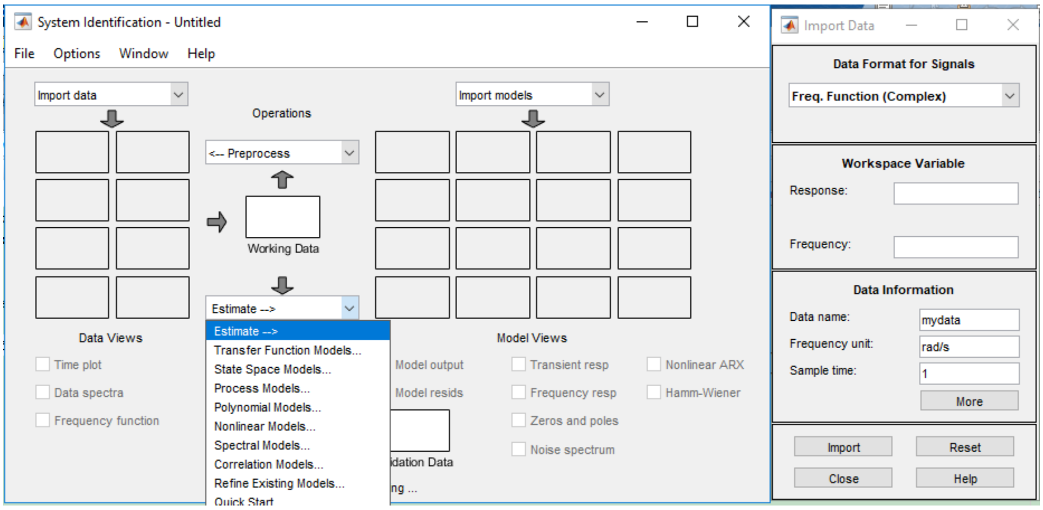

Figure 4.2: Matlab System Identification Toolbox provided an easier way for model development.

However, in our case, we observed in the Bode plot Fig 4.3 that although the gain plot fitting was reasonable, this initial canonical second order model couldn't fit the phase of ETFE very well because the ETFE had more phase lag especially at high frequencies. Then, instead, a better fitting would be accomplished if we introduced a delay term in the model. So, we finally modeled the system with a time-delayed transfer function of two poles and no zeros. We call this model as "The Canonical Second Order Transfer Function Model with Time Delay". In other words, our estimation of FRF for the refuge tracking system here was very similar to the original second order system, the only difference being that our model included a delay.

Then, this "The Canonical Second Order Transfer Function Model with Time Delay" model for the estimation of FRF G_{est1} of fish refuge tracking sys-

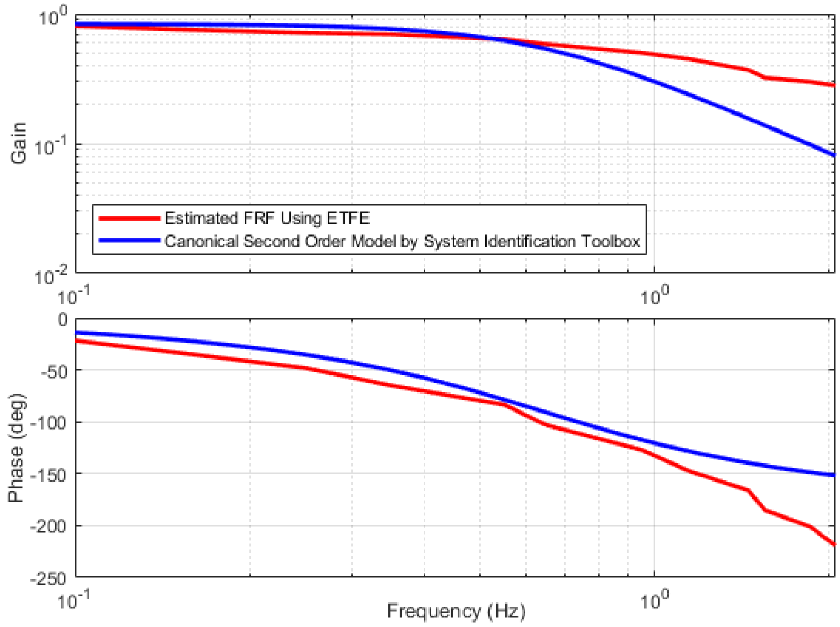

Figure 4.3: Comparison between the estimated FRF using ETFE (red color) and canonical second order model estimated by Matlab System Identification Toolbox (blue color) in Bode plot. Take model of one fish data (out of $N = 4$) as an example.

tem can be written as:

$$G_{est1}(s) = \frac{K_{dc}{\omega_n}^2}{s^2 + 2\xi\omega_n s + {\omega_n}^2} e^{-\tau s}. \tag{4.2}$$

The Bode plot in Fig 4.4 indicates the comparison between the non-parametric FRF estimation ETFE and the fitted "The Canonical Second Order Transfer Function Model with Time Delay" model using modeling for one fish data as illustration. The bad fitting in phase plot at high frequency was solved by this delay term. But one structural deficiency of this model is that it treats the delay as occurring as a feed forward (open-loop) term. Given the topology of

Fig. 1.2, the delay should really be included in the feedback, as in the next section.

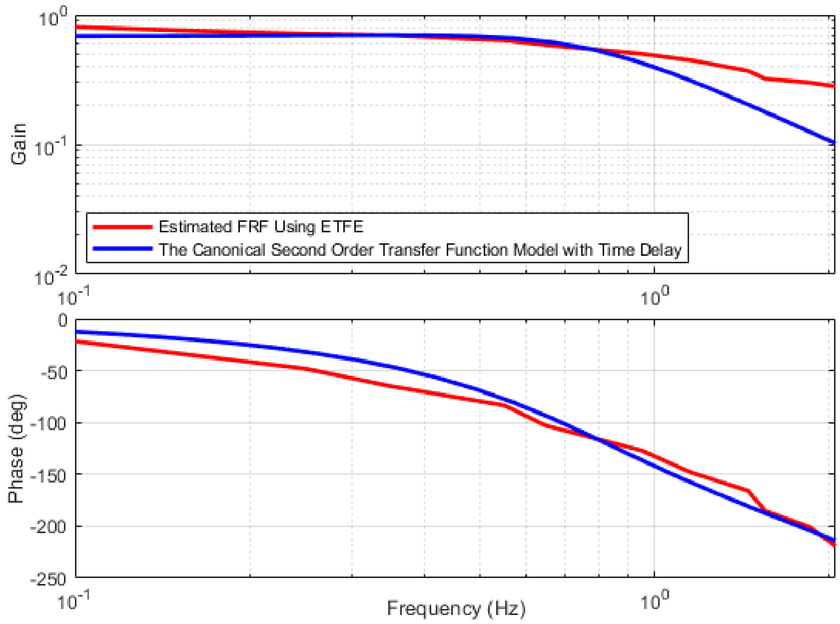

Figure 4.4: Comparison between the estimated FRF using ETFE (red color) and "The Canonical Second Order Transfer Function Model with Time Delay" (blue color) in Bode plot. Take model of one fish data (out of $N = 4$) as an example.

4.1.2 McRuer Crossover Model for Fish Refuge Tracking System FRF *G*

McRuer Crossover Model is a mathematical model of Human Pilot Behavior developed by Duane T. McRuer in 1974 [31]. Recent study has discovered that this model can be used to predict tracking response of *Eigenmannia virescens* [32]. The form of McRuer Crossover Model is typically like the Eq (4.3):

$$M(s) = \frac{K_p}{s} e^{-\tau s}. \tag{4.3}$$

This model includes a gain K_p, an origin pole and delay for a transfer function $M(s)$. In our case, we followed the procedure done in section 4.1.1, using the process models estimation in Matlab System Identification Toolbox. And we also manually tuned the parameters of the Matlab System Identification Toolbox fitting results to get a better model. Then we observed that this McRuer Crossover Model could fit the data-driven ETFE of fish refuge tracking system very well, and could be even improved when the pole location was not at the origin. Then, a more generalized form was used for our McRuer Crossover Model fitting, which no longer restricted the pole location to be zero. In that way, our McRuer Crossover Model for the estimation of refuge tracking system FRF G_{est2} became:

$$G_{est2}(s) = \frac{K_p}{s + p} e^{-\tau s}, \tag{4.4}$$

i.e. a lag filter with delay, instead of a pure integrator. We fitted this model with the ETFE and had the comparison in Bode plot Fig 4.5. From Fig 4.5, we could observe a very nice model fitting of ETFE by McRuer Crossover Models.

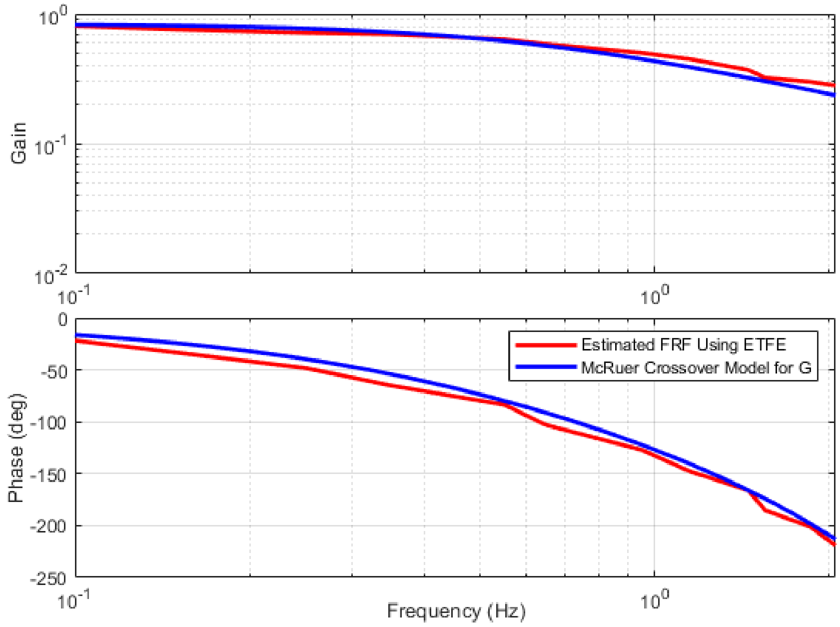

Figure 4.5: Comparison between the estimated FRF using ETFE (red color) and McRuer Crossover Model fitting with FRF *G* (blue color) in Bode plot. Take model of one fish data (out of $N = 4$) as an example.

4.1.3 McRuer Crossover Model for Fish Tracking System Inner Loop *CP*

From the second idea of parametric system identification, we could model the inner loop CP of refuge tracking system and calculate the FRF back using the Eq (4.5):

$$G(s) = \frac{C(s)P(s)}{1 + C(s)P(s)}. \tag{4.5}$$

Here, by observing the Bode plot of the inner loop CP for refuge tracking system, we also fitted it with McRuer Crossover Model. That was

$$CP_{est}(s) = \frac{K_p}{s+p}e^{-\tau s}. \tag{4.6}$$

Following the previous procedure to get an initial fitting in Matlab System Identification Toolbox and manually adjusted parameters for better model results, we got the final fitting result like the Fig 4.6 which indicated a good fitting.

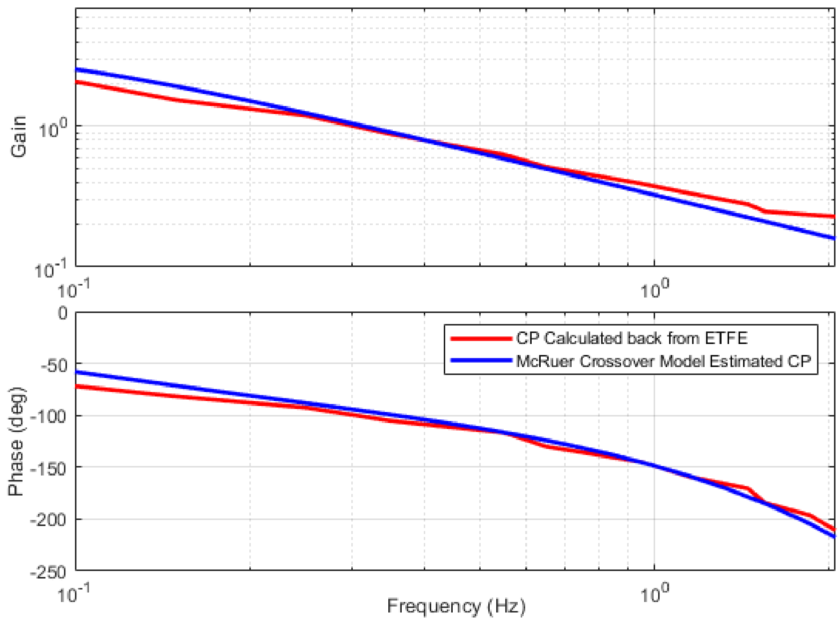

Figure 4.6: McRuer Crossover Model fitting with *CP*. Take model of one fish data (out of $N = 4$) as an example.

Then we calculated back using the Eq (4.5) for the estimation of the FRF of refuge tracking system G_{est3}, with the Bode plot in Fig 4.7.

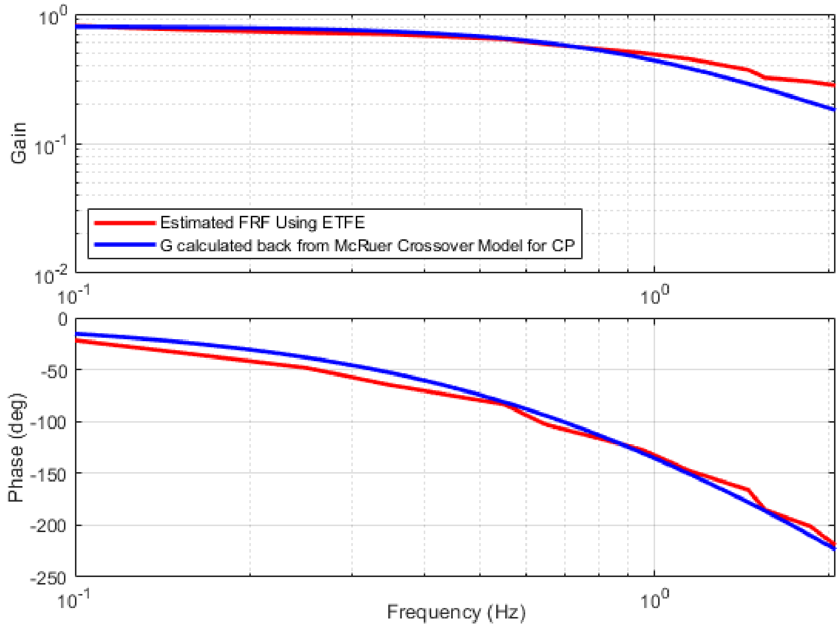

Figure 4.7: Refuge tracking system FRF G calculated back from McRuer Crossover Model for *CP*. Take model of one fish data (out of $N = 4$) as an example.

4.2 Discussion

In parametric system identification, we used three different models to represent the FRF of refuge tracking system.

As we can see from Fig 4.8, all of these three models can fit the non-parametric FRF estimate with ETFE very well for the sampled fish. The fitting graphs for all the fish ($N = 4$) are in the Fig 4.9 and parameters of each model fitting for these fish are in the Table 4.1. However, we do not currently have a quantative metric to judge which fitting method is best. We need strategies and methods that can evaluate the fitting (for example modeling consistency, fit error) so that we can easily decide which model provides the best fit for the refuge

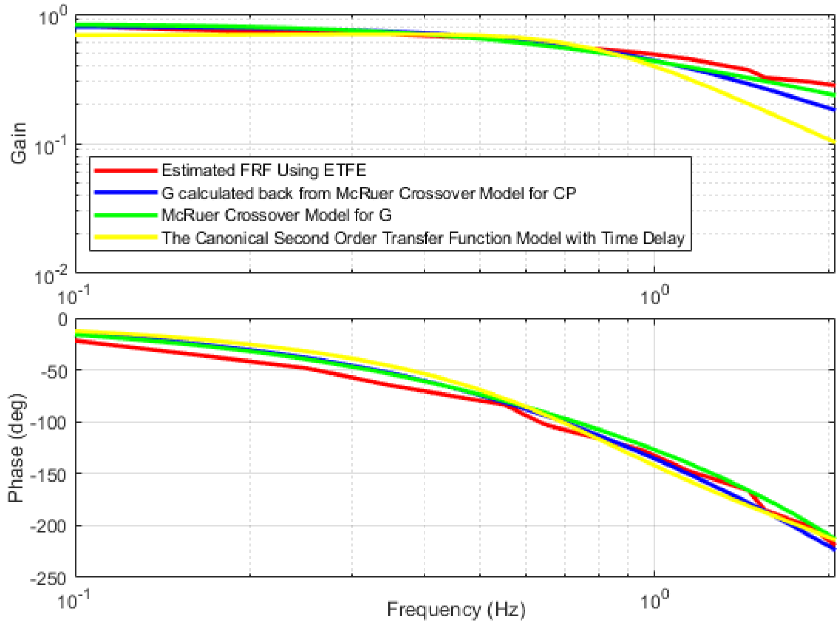

Figure 4.8: Comparison among three parametric system identification models and ETFE. The red, blue, green and yellow curves represent: the estimated G by ETFE, the parametric model of G calculated from the McRuer Crossover Model for CP, the McRuer Crossover Model for G, and the Canonical Second Order Transfer Function Model with Time Delay for G, respectively. Take model of one fish data (out of $N = 4$) as an example.

tracking system. This will become a significant part in our future work.

Model Type / Fish Name	The Canonical Second Order Transfer Function Model with Time Delay	McRuer Model for G	G Calculated back from McRuer CP
Gui	$\frac{15.2}{s^2+7.28s+28.80}e^{-0.10s}$	$\frac{2.74}{s+4.77}e^{-0.22s}$	$\frac{1.61e^{-0.18s}}{s+1.15+1.61e^{-0.18s}}$
Key	$\frac{16.6}{s^2+6.24s+24.28}e^{-0.09s}$	$\frac{3.17}{s+3.79}e^{-0.19s}$	$\frac{2.05e^{-0.18s}}{s+0.50+2.05e^{-0.18s}}$
Doc	$\frac{17.97}{s^2+8.69s+40.08}e^{-0.14s}$	$\frac{2.71}{s+5.76}e^{-0.22s}$	$\frac{1.42e^{-0.19s}}{s+1.22+1.42e^{-0.19s}}$
Luna	$\frac{11.3}{s^2+10.6s+18.54}e^{-0.10s}$	$\frac{1.02}{s+1.58}e^{-0.17s}$	$\frac{0.90e^{-0.14s}}{s+0.19+0.90e^{-0.14s}}$

Table 4.1: Parameters of three models with four fish.

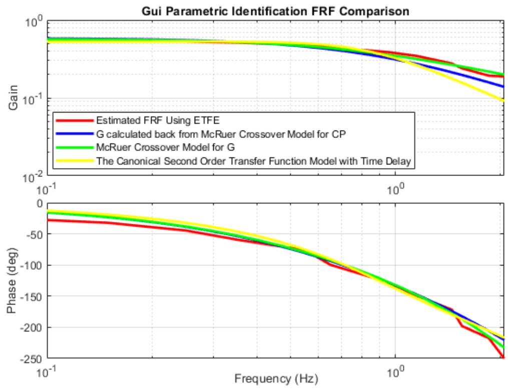

(a) "Gui" Parametric Comparison.

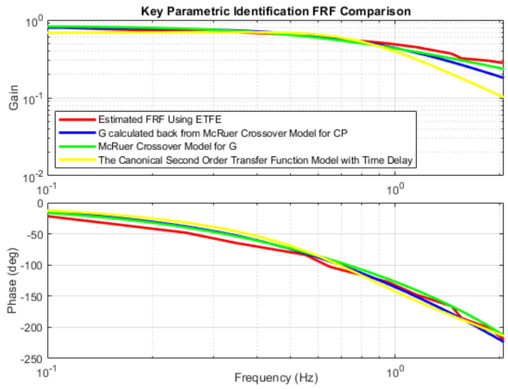

(b) "Key" Parametric Comparison.

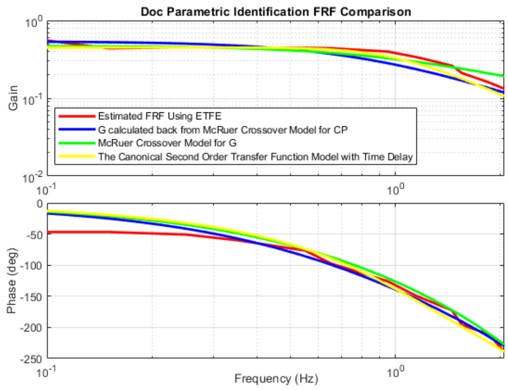

(c) "Doc" Parametric Comparison.

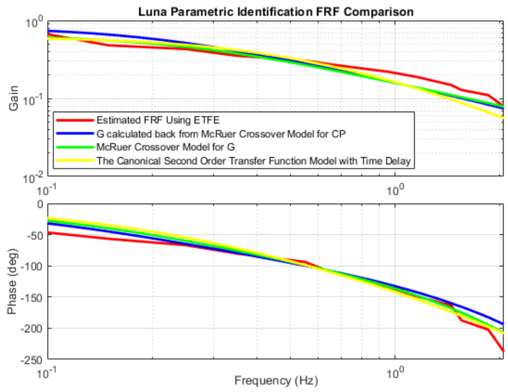

(d) "Luna" Parametric Comparison.

Figure 4.9: Comparison among three parametric system identification models and ETFE for $N = 4$ (fish name: Gui, Key, Doc and Luna). The estimates of G by ETFE for each fish is in red color, the "Canonical Second Order Transfer Function Model with Time Delay for G" is in yellow color, "Estimated G calculated back from McRuer Crossover Model for CP" is in blue color, "McRuer Crossover Model for G" is in green color.

Chapter 5

Conclusion and Future Works

In this study, we focused on comparing different system identification techniques for animal behavior – refuge tracking of *Eigenmannia virescens*. The techniques include non-parametric system identification and parametric system identification. In non-parametric system identification, we implemented both deterministic (sum of sines and chirp) and pseudo-stochastic (noise) input to analyze how the input signal affects the frequency response function estimation. In parametric system identification, we compared different parametric models to see how different mathematical models capture the animal behavior. Our finding is that for stochastic stimulus, fish didn't track the high frequency refuge movement very well. We were also not able to assess by visual inspection if the fish performed the behavior or not. The chirp stimulus has similar problems due to the frequency increasing and magnitude decreasing with time. But in sum of sines case fish presented the smoothest Bode plot and this case could be more accurate to be estimated by ETFE. So among all these three stimulus, the sum of sines seems to be the most practical and convenient input for us to study the fish tracking behavior. In parametric system identification, we found that the second order model with delay, the McRuer Crossover Model for FRF G and McRuer Crossover Model for Fish inner loop CP could capture the fish tracking behavior very well.

A natural next step is to develop a metric to evaluate the performance of the parametric models for model selection. Besides, various other system identification techniques can be tested to investigate if there are better techniques to be used for identifying the refuge tracking response of the weakly electric fish. Such techniques include but are not limited to using subspace-based state space identification techniques for example.

Bibliography

[1] M. J. Dunlop and R. M. Murray, "Towards biological system identification: fast and accurate estimates of parameters in genetic regulatory networks," *Parameters*, vol. 1000, p. 4, 2006.

[2] M. E. Csete and J. C. Doyle, "Reverse engineering of biological complexity," *Science*, vol. 295, no. 5560, pp. 1664–1669, 2002.

[3] R. J. Full and D. E. Koditschek, "Templates and anchors: Neuromechanical hypotheses of legged locomotion on land," *Journal of Experimental Biology*, vol. 202, no. 23, pp. 3325–3332, 1999.

[4] R. Blickhan, "The spring-mass model for running and hopping," *Journal of Biomechanics*, vol. 22, no. 11-12, pp. 1217–1227, 1989.

[5] C. R. Lee and C. T. Farley, "Determinants of the center of mass trajectory in human walking and running." *Journal of Experimental Biology*, vol. 201, no. 21, pp. 2935–2944, 1998. [Online]. Available: http://jeb.biologists.org/content/201/21/2935

[6] P. Holmes, R. J. Full, D. Koditschek, and J. Guckenheimer, "The dynamics of legged locomotion: Models, analyses, and challenges," *SIAM Review*, vol. 48, no. 2, pp. 207–304, 2006.

[7] I. Uyanik, Ö. Morgül, and U. Saranli, "Experimental validation of a feed-forward predictor for the spring-loaded inverted pendulum template," *IEEE Transactions on Robotics*, vol. 31, no. 1, pp. 208–216, 2015.

[8] A. K. Tangirala, *Principles of System Identification: Theory and Practice*. Crc Press, 2014.

[9] L. Ljung, Ed., *System Identification (2nd Ed.): Theory for the User*. Upper Saddle River, NJ, USA: Prentice Hall PTR, 1999.

[10] R. Pintelon and J. Schoukens, *System Identification: A Frequency Domain Approach*. John Wiley & Sons, 2012.

[11] K. J. Åström and P. Eykhoff, "System identificationa survey," *Automatica*, vol. 7, no. 2, pp. 123–162, 1971.

[12] P. Van Overschee and B. De Moor, *Subspace Identification for Linear Systems: Theory Implementation Applications*. Springer Science & Business Media, 2012.

[13] S. Haykin, *Neural Networks: A Comprehensive Foundation*. Prentice Hall PTR, 1994.

[14] I. Uyanik, S. A. Stamper, N. J. Cowan, and E. S. Fortune, "Sensory cues modulate smooth pursuit and active sensing," *Frontiers in Behavioral Neuroscience*, vol. 13, p. 59, 2019.

[15] E. Roth, K. Zhuang, S. A. Stamper, E. S. Fortune, and N. J. Cowan, "Stimulus predictability mediates a switch in locomotor smooth pursuit performance for *Eigenmannia virescens*," *Journal of Experimental Biology*, vol. 214, no. 7, pp. 1170–1180, 2011.

[16] N. J. Cowan and E. S. Fortune, "The critical role of locomotion mechanics in decoding sensory systems," *Journal of Neuroscience*, vol. 27, no. 5, pp. 1123–1128, 2007.

[17] S. A. Stamper, E. Roth, N. J. Cowan, and E. S. Fortune, "Active sensing via movement shapes spatiotemporal patterns of sensory feedback," *Journal of Experimental Biology*, vol. 215, no. 9, pp. 1567–1574, 2012.

[18] M. Markham, Y. Ban, A. McCauley, and R. Maltby, "Energetics of sensing and communication in electric fish: A blessing and a curse in the anthropocene?" *Integrative and Comparative Biology*, vol. 56, no. 5, p. 889, 2016.

[19] T. H. Bullock, C. D. Hopkins, and R. R. Fay, *Electroreception*. Springer Science & Business Media, 2006, vol. 21.

[20] E. W. Tan, J. M. Nizar, E. Carrera-g, and E. S. Fortune, "Electrosensory

interference in naturally occurring aggregates of a species of weakly electric fish, *Eigenmannia virescens*," *Behavioural Brain Research*, vol. 164, no. 1, pp. 83–92, 2005.

[21] E. E. Sutton, A. Demir, S. A. Stamper, E. S. Fortune, and N. J. Cowan, "Dynamic modulation of visual and electrosensory gains for locomotor control," *Journal of The Royal Society Interface*, vol. 13, no. 118, p. 20160057, 2016.

[22] S. Sefati, I. D. Neveln, E. Roth, T. R. Mitchell, J. B. Snyder, M. A. MacIver, E. S. Fortune, and N. J. Cowan, "Mutually opposing forces during locomotion can eliminate the tradeoff between maneuverability and stability," *Proceedings of the National Academy of Sciences*, vol. 110, no. 47, pp. 18 798–18 803, 2013.

[23] S. Sefati, I. Neveln, M. A. MacIver, E. S. Fortune, and N. J. Cowan, "Counter-propagating waves enhance maneuverability and stability: a bio-inspired strategy for robotic ribbon-fin propulsion," in *2012 4th IEEE RAS & EMBS International Conference on Biomedical Robotics and Biomechatronics (BioRob)*. IEEE, 2012, pp. 1620–1625.

[24] I. Uyanik, S. Sefati, S. A. Stamper, K.-A. Cho, M. M. Ankarali, E. S. Fortune, and N. J. Cowan, "Variability in locomotor dynamics reveals the critical role of feedback in task control," *Elife*, vol. 9, p. e51219, 2020.

[25] D. Biswas, L. A. Arend, S. A. Stamper, B. P. Vágvölgyi, E. S. Fortune, and N. J. Cowan, "Closed-loop control of active sensing movements regulates sensory slip," *Current Biology*, vol. 28, no. 24, pp. 4029–4036, 2018.

[26] F. Pedraja, V. Hofmann, K. M. Lucas, C. Young, J. Engelmann, and J. E. Lewis, "Motion parallax in electric sensing," *Proceedings of the National Academy of Sciences*, vol. 115, no. 3, pp. 573–577, 2018.

[27] É. M. Hitschfeld, S. A. Stamper, K. Vonderschen, E. S. Fortune, and M. J. Chacron, "Effects of restraint and immobilization on electrosensory behaviors of weakly electric fish," *ILAR Journal*, vol. 50, no. 4, pp. 361–372, 2009.

[28] K. T. Yoshida, I. Uyanik, E. Sutton, and N. J. Cowan, "A new experimental system to test how the brain learns novel locomotion dynamics," in *Integrative and Comparative Biology*, vol. 58. Oxford Univ Press Inc Journals Dept, 2001 Evans Rd, Cary, NC 27513 USA, 2018, pp. E455–E455.

[29] I. Uyanik, M. M. Ankaralı, N. J. Cowan, U. Saranlı, and Ö. Morgül, "Identification of a vertical hopping robot model via harmonic transfer functions," *Transactions of the Institute of Measurement and Control*, vol. 38, no. 5, pp. 501–511, 2016.

[30] D. Logan, T. Kiemel, and J. J. Jeka, "Using a system identification ap-

proach to investigate subtask control during human locomotion," *Frontiers in Computational Neuroscience*, vol. 10, p. 146, 2017.

[31] D. T. McRuer and E. S. Krendel, "Mathematical models of human pilot behavior," Advisory Group for Aerospace Research and Development Neuilly-sur-Seine (France), Tech. Rep., 1974.

[32] B. Nixon, I. Uyanik, Y. Yang, and N. J. Cowan, "Sensory salience affects sensorimotor delay in the tracking response of the glass knifefish," in *Integrative and Comparative Biology*, vol. 59. Oxford Univ Press Inc Journals Dept, 2001 Evans Rd, Cary, NC 27513 USA, 2019, pp. E378–E378.

Vita

Yu Yang received his B.S. degree in Electrical Engineering and Automation from Harbin Institute of Technology, China in 2016, and enrolled in the Electrical and Computer Engineering M.S.E. program at Johns Hopkins University in 2017. He is currently associated with Dr. Noah Cowan′s Locomotion in Mechanical and Biological Systems (LIMBS) Laboratory, Johns Hopkins University. His research interests include System Identification of Refuge tracking system for weakly electric glass knifefish and how sensory salience affects the tracking response of these fish.